



Pressurization Characteristics of a Piezoelectric-Hydraulic Pump for UAV Brake Systems

Jai-Hyuk Hwang¹ · Jae-Sung Bae¹ · Yong-Ha Hwang² · Jun-Yong Kwon³

Received: 16 July 2017 / Revised: 12 February 2018 / Accepted: 23 April 2018 / Published online: 9 August 2018
© The Korean Society for Aeronautical & Space Sciences and Springer Nature Singapore Pte Ltd. 2018

Abstract

In this paper, a small piezoelectric-hydraulic pump suitable for the braking system of small- and medium-sized UAVs was developed. In addition, the pressurization characteristics of the pump were analyzed and performance experiments of the developed pump were conducted. To analyze the pressurization characteristics, AMESim, a verified commercial program, was used. The modeling of the small piezoelectric-hydraulic pump was carried out by subdividing it into components, including the piezoelectric actuator, chamber, check valves, and load side. The modeling validity was confirmed via a comparison of the simulation results with the performance experimental results of the produced pump. It has been found that the simulations and experiments produced similar results regarding the overall pressurization characteristics.

Keywords Piezoelectric-hydraulic pump · Piezoelectric actuator · Check valve · UAV brake system

1 Introduction

Generally, aircraft employ hydraulic systems that use the pressure of a hydraulic fluid as their power transmission medium. These systems are reliable, economical and safe, not to mention its certainty of operation and compact structural design. Aircraft braking systems that use general hydraulic systems require complicated parts such as hydraulic reservoirs, servo valves, check valves, and electronic control devices. However, in the case of UAVs, space constraints and system complexity make it difficult to apply hydraulic pressure. In particular, most small- and medium-sized UAVs currently in use do not use hydraulic pressure for applications other than braking systems, and general hydraulic systems are considered inefficient for UAV braking systems. Therefore, it is necessary to study a small hydraulic pump that can supply the necessary hydraulic pressure for

a brake hydraulic system and develop miniaturized and efficient hydraulic brake system technologies [1–4].

A small hydraulic pump requires various hydraulic components, including a chamber, actuator, check valves, and hydraulic circuit. Among them, the actuator accounts for the largest ratio in efficiency and size. In developing this miniaturized efficient hydraulic pump, selecting the actuator is critical in that a small but powerful actuator is needed. Regarding actuator technology, several types of smart materials have been studied recently. The most suitable of these materials for small hydraulic pumps is piezoelectric ceramic (PZT) [4–7]. By applying a compact smart material pump that uses a piezoelectric actuator as a drive source to a brake hydraulic circuit, the size and weight of the brake system can be significantly reduced. This is highly advantageous for UAVs where space and weight are limited.

In the present study, a small piezoelectric-hydraulic pump was developed to satisfy the brake system requirements of small- and medium-sized UAVs. These requirements included the exhaust flow rate, high pressure, fast response speed, and stable operation. The pressurization characteristics of the pump were analyzed and performance experiments were conducted. Piezoelectric ceramic actuators can generate greater force than other smart material actuators and can operate at high speed, but suffer from a very small mechanical displacement. When the mechanical displacement is small, the exhaust flow rate of the pump decreases. There-

✉ Jai-Hyuk Hwang
jhhwang@kau.ac.kr

¹ Department of Aerospace and Mechanical Engineering, Aerospace University, Gyeonggi 10540, Korea

² Department of Aerospace and Mechanical Engineering, Graduate School at KAU, Gyeonggi 10540, Korea

³ The 7th Research and Development Institute, Agency for Defense Development, Daejeon 34186, Korea

fore, it is necessary to design a sophisticated check valve that effectively discharges the small flow rate of the piezoelectric-hydraulic pump in a single direction. For the present study, a small sheet spring type check valve was designed to effectively transmit the small flow rate in the output direction. In this case, the check valve had to be able to adapt well to the high-speed operation of the piezo-ceramic actuator. The passive check valve was used to reduce the complexity of the system to meet the light weight and miniaturization objectives of the study. The small piezoelectric-hydraulic pump was able to increase the driving speed and obtain the required flow rate even though the exhaust flow rate was small [8–11].


In this paper, to analyze the pressurization characteristics of the compact piezoelectric-hydraulic pump, the AMESim program was used. The hydraulic pump components—the piezoelectric actuator of the piezoelectric-hydraulic pump, the chamber, the check valves, and the load—were analytically modeled. The AMESim simulation results were compared with the designed piezoelectric-hydraulic pump's performance experiment results. The technical model was used rather than a single component to enable elaborate modeling for the dynamic characteristics of the check valves from the AMESim program. The flow path through the check valve to the end of the load was modeled with a pipeline instead of a simple flow path to obtain more accurate simulation results. In addition, the performance experiments of the produced pump confirmed that it could be applied to the brake systems of small- and medium-sized UAVs. To the authors' knowledge, research on piezoelectric-hydraulic pumps applied to small- and medium-sized UAVs is thus far absent in the literature. Accordingly, the results of the present research are considered to be the first attempt.

2 Design of Piezoelectric-Hydraulic Pump for a Brake System

Aircraft brakes are devices that convert the kinetic energy at landing into thermal energy due to the friction of the disk brake, thereby stopping the movement of the aircraft [12]. In this study, a lightweight single-engine aircraft with similar weight and performance characteristics to those of small- and medium-sized UAVs was selected as a target aircraft with reference to the FAA Handbook. The main design variables of the aircraft brake system included the weight of the aircraft, the braking speed, the number of main wheels, the required braking distance, and deceleration. Therefore, using the specifications of the selected aircraft, the requirements of the brake system were analyzed. The detailed specifications are shown in Table 1 [13, 14].

Braking pressure can be divided into static pressure and dynamic pressure. Static pressure is the pressure to maintain a stopped state when the engine is in operation or when the

Table 1 Specifications of a target airplane



Parameters	Value
Max. take-off weight [MTOW]	5862 lb
Design landing weight [DLW]	4000 lb
Stall speed	
MTOW	70 knots
DLW	65 knots
Deceleration rate	
Normal	6 ft/s ²
RTO	10 ft/s ²
Radius of tires	7.88 inch
Number of main tires	2 inch

Table 2 Design requirements of piezoelectric-hydraulic pump

Parameters	Value
Normal operating pressure	450–500 psi
Outlet flow rate	≥ 0.02 cc/stroke
Response time	≤ 30 ms
Operation speed	120–150 Hz

aircraft is stopped. Dynamic pressure is the pressure needed for the aircraft to stop at landing. It is also the greater of the two pressures. Based on this value, the normal operating pressure of the pump was calculated.

The braking energy was calculated under the condition of the design landing weight (DLW) based on the specification of the aircraft to be designed, assuming that the aircraft's stall speed of 65 knots was the landing speed of the aircraft. The normal operating pressure of the pump was chosen to be about 450 psi considering the DLW and braking energy [15]. The flow requirement is a value that varies according to the distance between the brake pad and the disk. The exhaust flow rate of the piezoelectric-hydraulic pump designed in this study was set to 0.02 cc for a design flow rate per stroke, considering the expansion of the hydraulic pipe in part when the brake pad would be in contact with the disk. The response time for the piezoelectric-hydraulic pump to form the hydraulic pressure was selected to be 30 ms in consideration of the ABS function of the brake system [15, 16]. Finally, since the piezoelectric actuator would operate at high speed, an operating frequency range of 120–150 Hz was selected. The design requirements of the piezoelectric-hydraulic pump developed in this study are shown in Table 2.

The piezoelectric-hydraulic pump in this study used a piston-type pump mechanism and performed four

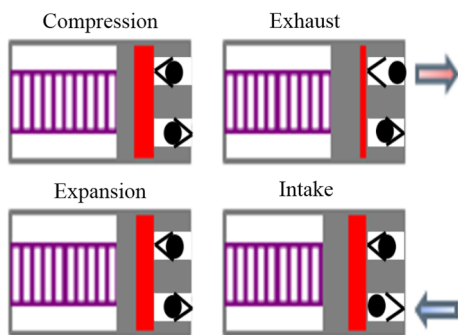


Fig. 1 Sequences of piston-type pumping mechanism

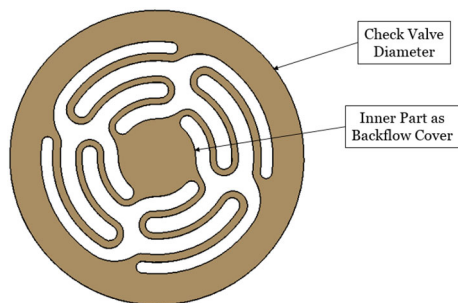


Fig. 2 Shape of sheet-spring type check valve

operational stages—compression, exhaust, expansion, and intake—according to the voltage applied to the piezoelectric actuator, causing pressure to build up on the load side. Figure 1 shows a schematic diagram with the piston-type pump mechanism [7, 17].

In the compression process, with both check valves closed, the pressure inside the chamber rises due to the mechanical displacement of the stacked piezoelectric actuator. In the exhaust process, when the pressure in the chamber becomes greater than the cracking pressure of the exhaust port side check valve, the exhaust port check valve is opened so that the flow goes out through the exhaust port. In the expansion process, with both check valves closed, the pressure in the chamber decreases due to the contraction of the stacked piezoelectric actuator. In the intake process, when the pressure inside the chamber becomes smaller than the cracking pressure of the inlet side check valve, the check valve of the inlet side opens, and the fluid is sucked into the chamber. Through the pumping process of these four steps, the fluid in the inlet port can be pumped toward the exhaust port.

In this study, the check valve adopted for the piezoelectric-hydraulic pump was a passive sheet-spring type check valve that could move according to the high-speed operation of the piezoelectric actuator. Its shape is shown in Fig. 2 [8].

The check valve is an indispensable part of the piezoelectric-hydraulic pump and is designed to be able to effectively block the backflow of the fluid under the high-speed operation conditions of the piezoelectric actuator. In

this study, the designed check valve was composed of an inner section that restricted the flow of hydraulic fluid, and a fixed outer section. The spring stiffness of the check valve can be changed according to the dimension of the legs and the material property value. In the preceding study, the dimension, the material property, and the shape of the check valve were determined through the parametric study to meet its operating requirements [9–11]. The natural frequency of the check valve was designed to have a structure–fluid coupled natural frequency of 400 Hz or more so that it did not affect the operation speed of the piezoelectric-hydraulic pump.

The diameter of the pump chamber, which affected the exhaust characteristics of the piezoelectric-hydraulic pump, was theoretically calculated through mathematical modeling and applied to the shape design [17, 18]. The exhaust pressure, P , of the piezoelectric-hydraulic pump indicated the pressure generated inside the chamber, and is expressed by Eq. (1).

$$P = \frac{F_{\text{total}}}{A_{\text{ch}}} = \frac{F_b - x_p K_{\text{ch}}}{A_{\text{ch}}}, \quad (1)$$

where F_b is the maximum driving force of the stacked piezoelectric actuator, x_p is the distance the piston actually moved, A_{ch} is the area of the chamber, and K_{ch} is the stiffness of the fluid in the chamber. x_p and K_{ch} could be calculated using Eqs. (2) and (3).

$$x_p \frac{K_{\text{stack}}}{K_{\text{stack}} + K_{\text{ch}}} x_{\text{free}} \quad (2)$$

$$K_{\text{ch}} = \frac{\beta A_{\text{ch}}}{L_{\text{ch}}}, \quad (3)$$

where K_{stack} is the stiffness of the piezoelectric actuator, x_{free} is the maximum displacement of the piezoelectric actuator, β is the bulk modulus of the working fluid, and L_{ch} is the height of the chamber. Further, the actual exhaust flow rate of the piezoelectric-hydraulic pump, Q , could be obtained using the area of the chamber, A_{ch} , the displacement of the piston by the stacked piezoelectric actuator, x_p , and the operating frequency, f , as shown in Eq. (4).

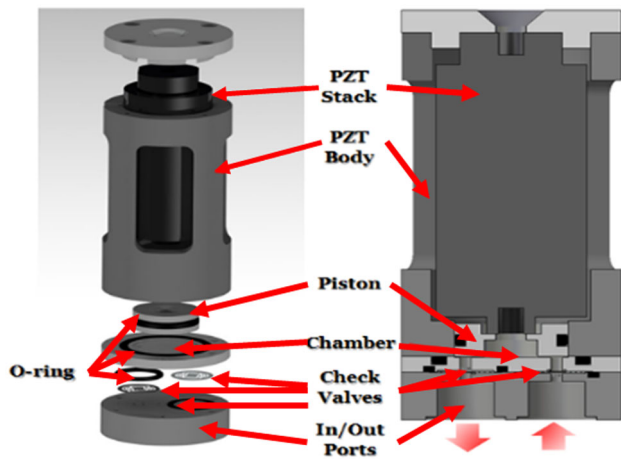
$$Q = 60 A_{\text{ch}} \cdot x_p \cdot f. \quad (4)$$

To satisfy the requirements of Table 2 obtained based on the calculation results, a piezoelectric actuator (P-225.40, PI Company) was selected for the piezoelectric-hydraulic pump. The selected actuator had a maximum force of 12,500 N and a maximum displacement of 60 μm at a maximum operating voltage of 1000 V. Detailed specifications are shown in Table 3.

The detailed shape of the designed piezoelectric-hydraulic pump is shown in Fig. 3 and the dimensions are summarized in Table 4. The structure of the piezoelectric-hydraulic

Table 3 Parameters of piezostack (PZT) actuator

Parameters	Value
Size	∅ 39.8 mm, <i>L</i> 94 mm
Max. displacement	60 μm
Blocked force	12,500 N
Capacitance	1300 nF
Stiffness	200 N/μm
Operating voltage	0–1000 V

**Fig. 3** Configurations of the piezoelectric-hydraulic pump**Table 4** Dimensions of the piezoelectric-hydraulic pump

Parameters	Dimension
Total length	<i>L</i> 128 mm
Cap	∅ 58 mm, <i>t</i> 7.6 mm
Case diameter	∅ 54.8 mm
Piston	∅ 30 mm, <i>t</i> 11.9 mm
Chamber	∅ 30 mm, <i>t</i> 0.5 mm
Check valve	∅ 19 mm, <i>t</i> 0.2 mm

pump included a stacked piezoelectric actuator, a piston, two check valves, and a housing, as shown in Fig. 3. O-rings were installed where components such as the check valves and the piston would make contact with the fluid to prevent the hydraulic pressure from being lost.

3 Pressurization Simulation of the Piezoelectric-Hydraulic Pump

The modeling of the piezoelectric-hydraulic pump was largely divided into the modeling of the major components such as the piezoelectric actuator, hydraulic chamber, check valves, and solenoid valve. AMESim, a widely used commercial program for hydraulic modeling, was used. The purpose

of the AMESim modeling is to predict the dynamic behavior of the piezoelectric-hydraulic pump using a simulation. In addition, the parameters affecting the dynamic characteristics of the piezoelectric-hydraulic pump are analyzed and applied to the pump design to improve its performance effectively. The cross-sectional area of the piezoelectric-hydraulic pump piston along with the stroke of the piezoelectric actuator will influence discharge flow per stroke. The dimensions of the pump chamber also affect the load pressure formed by piezoelectric actuators. Larger piston cross section will result in larger discharge flow rate, but lower load pressure formation. Therefore, using the AMESim modeling, an optimal piston cross-section and chamber dimensions were selected in order for the flow rate and load pressure to meet the requirements of the brake system. Furthermore, the piezoelectric-hydraulic pump design was validated by comparing the results of the AMESim simulation and the pump experiment. The AMESim model of the piezoelectric-hydraulic pump circuit is shown in Fig. 4.

To analyze the pressurizing behavior characteristics of the small-sized piezoelectric-hydraulic pump, it was necessary to model the piezoelectric actuator first. After setting the parameter value of the piezoelectric actuator, the input voltage with the frequency was applied and the displacement of the actuator was obtained. The responses of the actuator with input values of 1000 V and 120 Hz using AMESim are shown in Fig. 5. This result matched the given data sheet of the piezoelectric actuator (P-225.40), thus confirming that the actuator modeling was suitable.

The pressurization simulation results for the load side using the designed AMESim model are shown in Fig. 6. The time to reach 450 psi, which is the normal operating pressure of the load part, was about 30 ms. This result satisfied the pump's requirement given in Table 2. The hydraulic chamber modeling was conducted using the corresponding components to the piston mass and the fluid chamber. The inlet check valve was modeled to suck fluid from the hydraulic reservoir when the piezoelectric actuator was in operation and prevent the reverse flow of fluid that entered from the hydraulic reservoir. The cracking pressure of the inlet check valve was set at 0.5 atm.

For the check valve of the exhaust port, it is necessary to transmit the pressure of the chamber to the load side when operating the piezoelectric actuator. In addition, to elaborately model the dynamic characteristics of the check valve, a flapper valve, mass, and spring components were used instead of a single component. The flow path through the check valve to the solenoid valve was also modeled with a pipeline, and the solenoid valve was modeled for the pressurization characteristics of the hydraulic pump. By turning off the solenoid valve, it is possible to close the hydraulic circuit and simulate the pressurization characteristics. Open-

Fig. 4 AMESim modeling for piezoelectric-hydraulic pump system

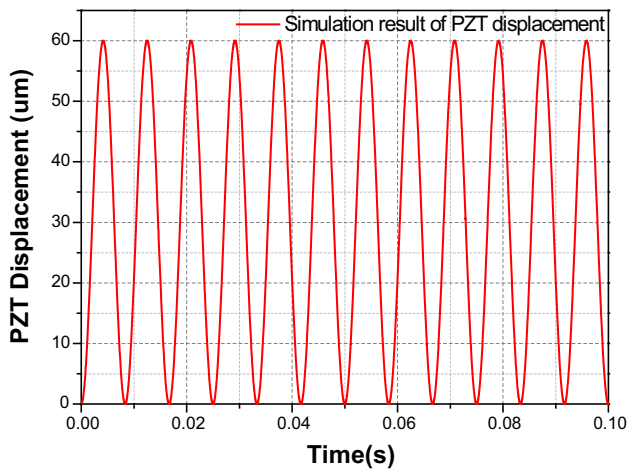
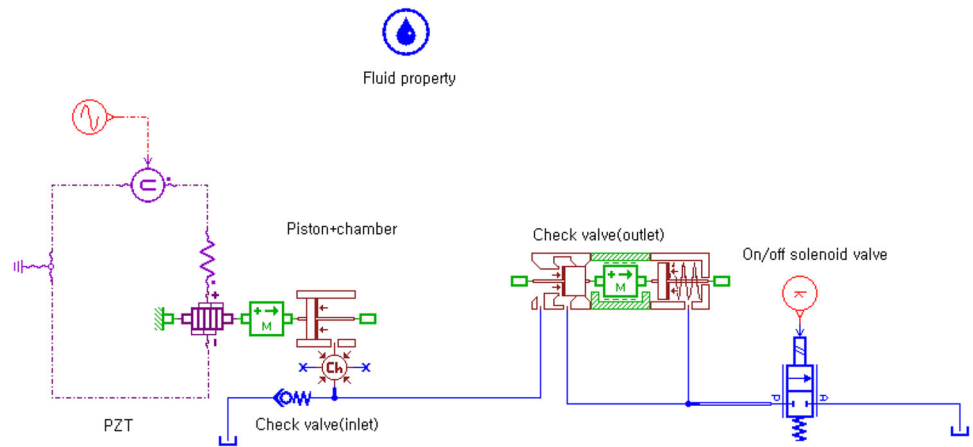


Fig. 5 Simulation of piezostack actuator displacement

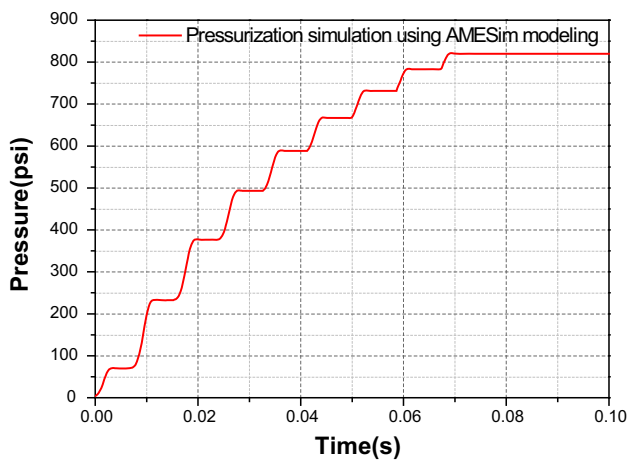


Fig. 6 Simulation of pressurization characteristics at load side (900 V, 120 Hz)

ing the solenoid valve enables an open hydraulic circuit to be formed.



Fig. 7 Components of the piezoelectric-hydraulic pump

4 Performance Test of the Manufactured Piezoelectric-Hydraulic Pump

In order to verify the performance of the designed piezoelectric-hydraulic pump, an actual piezoelectric-hydraulic pump, shown in Fig. 7, was manufactured based on the design results. The various parts of the designed piezoelectric-hydraulic pump were modularized to facilitate part replacement.

Components were manufactured via precision machining, and the check valves were made using wire-cut electric discharge machining because they were thin and complicated in shape. The produced parts of the piezoelectric-hydraulic pump are shown in Fig. 7.

For the performance test of the manufactured piezoelectric-hydraulic pump, the experimental devices such as a DAQ program, high voltage amplifier, pressure sensor, needle valve, and electronic scale were constructed, as shown in Fig. 8. The pressure sensor, Model A-10 of WIKA Corporation, was used for pressure measurement. The pressure sensor has a Wheatstone bridge to read the

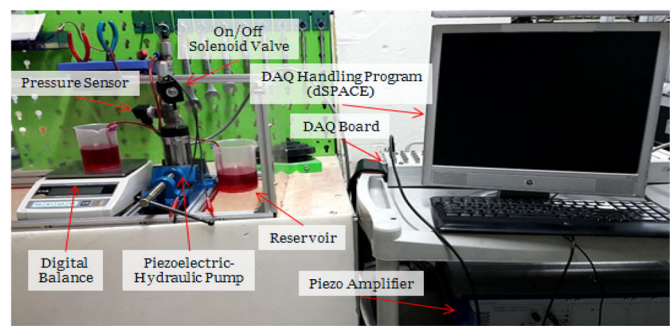
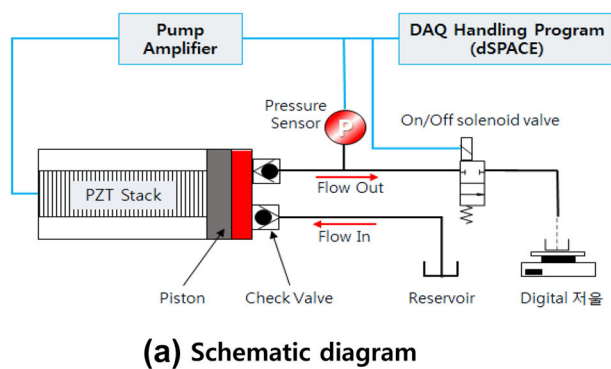


Fig. 8 Experimental schematic and setup

change of the resistances installed inside it. The output of the bridge is proportional to the applied pressure, and the input signal of 0–250 bar produces the output signal of 4–20 mA. The DAQ program used ‘dSPACE’ and was able to collect and create the digital and analog signal data. The high voltage amplifier amplified the generated signal and applied it to the piezoelectric actuator at a given driving speed. To obtain the high voltage output at the required driving frequency of 150 Hz, the E-481 model from PI Company was used.

The needle valve connected to the exhaust port of the piezoelectric-hydraulic pump played an important role in the exhaust performance test of the piezoelectric-hydraulic pump. When the needle valve was opened, the flow rate in the no-load state could be measured. If the needle valve was blocked, a closed-loop hydraulic circuit such as that in a brake system formed. The pressure of the exhaust port could be measured using a pressure sensor. In addition, Mil-PRF-83282, generally used in actual aircraft hydraulic brake systems, was used as the hydraulic fluid.

To determine the flow characteristics of the piezoelectric-hydraulic pump, no-load flow experiments were conducted according to the following process. First, the needle valve connected to the exhaust port was opened, and the flow rate after passing through the needle valve was measured using an electronic scale. With the zero point of the electronic scale aligned, a sin wave input, which had the driving frequency of the stacked piezoelectric actuators, was applied for 30 s to obtain the exhaust flow rate in the no-load state. At each time point, the peak value of the driving voltage was kept constant at 900 V. For the accuracy of the experimental data, the average value of the results obtained from several repeated experiments was used.

The graph in Fig. 9 shows the no-load exhaust flow rate of the piezoelectric pressure pump according to the operating frequency. The experimental results show that the exhaust flow increased linearly up to 80 Hz and converged to a constant value. The exhaust flow rate most likely converged as a

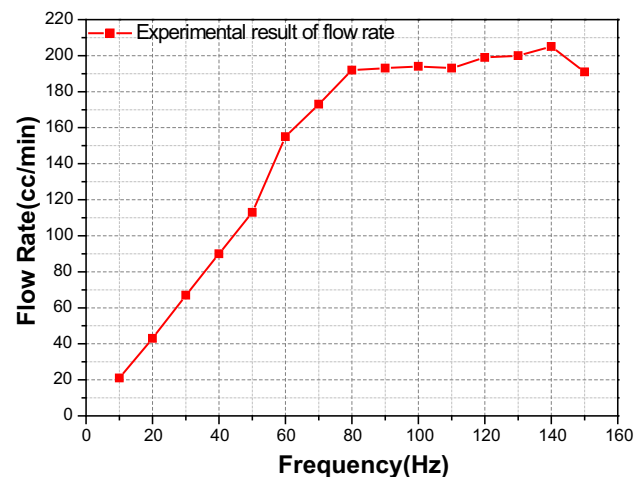


Fig. 9 Experimental results of pump outlet flow rate (no-load pressure)

result of the piston inertia, fluid inertia, and operating characteristics of the check valve. The maximum no-load exhaust flow rate was 205 cc/min at 140 Hz.

The experiments on the pressurizing characteristics for the manufactured piezoelectric-hydraulic pump were carried out according to the following process. First, the on/off solenoid valve connected to the exhaust port of the stacked piezoelectric-hydraulic pump was closed. Once the solenoid valve was closed, the flow path from the check valve of the exhaust port of the piezoelectric-hydraulic pump to the solenoid valve formed a closed-loop hydraulic circuit such as that in a brake system. Next, the input voltage was subsequently applied to the stacked piezoelectric actuator while changing the driving frequency. Then, the hydraulic pressure at the load side behind the exhaust port of the piezoelectric-hydraulic pump was measured using a pressure sensor. As in the exhaust flow measurement experiment, the operating frequency was changed from 10 to 150 Hz in units of 10 Hz while the driving voltage was kept constant at 900 V.

The measurement value of the hydraulic pressure at the load side for the stacked piezoelectric-hydraulic pump

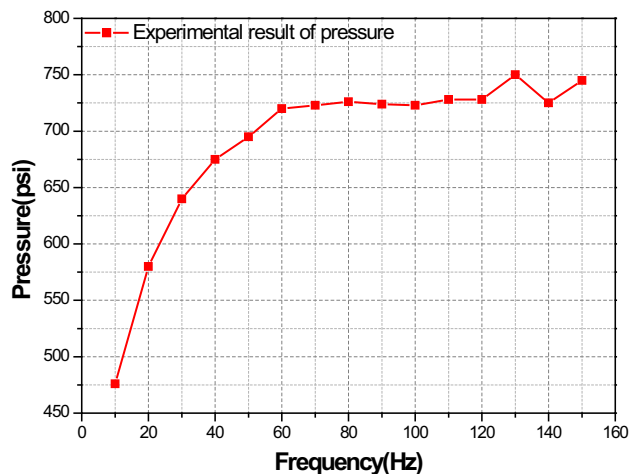


Fig. 10 Experimental results of pump outlet pressure (with closed loop)

according to the change in operating frequency is shown in Fig. 10. As the operating frequency increased, the hydraulic pressure at the load side increased. Using this result, it was determined that as the operating frequency increased, the pressurization characteristics of the stacked piezoelectric actuator and the check valve could be obtained more effectively. The maximum hydraulic pressure at the load side occurred at 130 Hz and 750 psi.

The flow rate and load pressure from the existing piezoelectric-hydraulic pumps are between 3 and 450 cc/min and 3–100 psi, respectively [1–4]. The piezoelectric-hydraulic pump designed in this paper has a flow rate of 205 cc/min with a load pressure of up to 750 psi. Although the flow rate is about medium compared to the existing piezoelectric-hydraulic pumps, the load pressure is very high. This shows that the piezoelectric-hydraulic pump of this study was developed for the brake system. The discharge flow rate of the piezoelectric-hydraulic pump developed in this study is sufficient to compress the brake hydraulic closed circuit within the required time to form the load pressure. The piezoelectric-hydraulic pump applied for a brake system requires the ability to form the load pressure even more than the flow rate. The ability of the existing piezoelectric-hydraulic pumps to form the load pressure does not meet the requirements of the brake system and, therefore, cannot be applied to the brake system. However, experiment and simulation have confirmed that the piezoelectric-hydraulic pump developed in this paper can form the load pressure beyond the normal operating pressure required by the brake system. As a result, it is deemed that the piezoelectric-hydraulic pump in this study is effectively applicable to the small- and medium-sized UAV braking systems.

Figure 11 compares the AMESim simulation results and actual experimental results on the process of forming the hydraulic pressure at the load behind the exhaust port of the

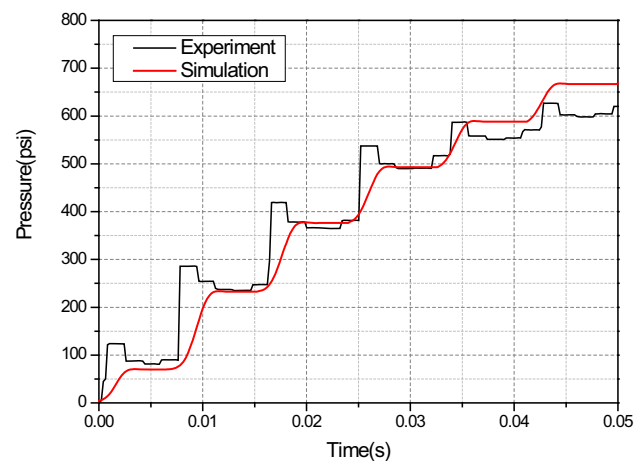


Fig. 11 Comparison of pressurization characteristics at load side (experiment vs simulation)

piezoelectric-hydraulic pump. The experimental results in Fig. 11 were obtained by measuring the process in which the hydraulic pressure at the load behind the pump exhaust port accumulated when the piezoelectric-hydraulic pump was driven at the operating frequency of 120 Hz. The time to reach the normal operating pressure (450 psi) required to operate the brakes was within about 30 ms, which matched the simulation results. In the AMESim simulation results, there was a slight difference in values compared to the experimental results of the actual hydraulic pump during the pressurization stage. This occurred because the fluid structure interaction (FSI) dynamic behavior of the check valve and its shape were not considered in the model. Therefore, for more accurate modeling, the FSI dynamic behavior and the check valve shape had to be included in the simulation model. In addition, in the case of the actual piezoelectric-hydraulic pump, fluctuations occurred in the pressure graph due to the imperfect seal of the check valve. However, it was impossible for the check valves to perfectly synchronize with the piezoelectric actuator without the leakage from the intake and exhaust unit. Therefore, by comparing the average value of the fluctuation occurring at every step with the simulation results, it was confirmed that the AMESim modeling was done properly.

In addition, the relation between the input voltage to the piezoelectric-hydraulic pump versus the hydraulic pressure at the load behind the exhaust port was measured experimentally. The results are shown in Fig. 12. Several experiments were conducted to increase the reliability of the results, and the mean value was used. The simulation results using AMESim for the relationship between the input voltage and the load pressure are also shown in Fig. 12. Comparing the simulation results and the experimental results, it was found that both results were very consistent and that the AMESim modeling was performed properly.

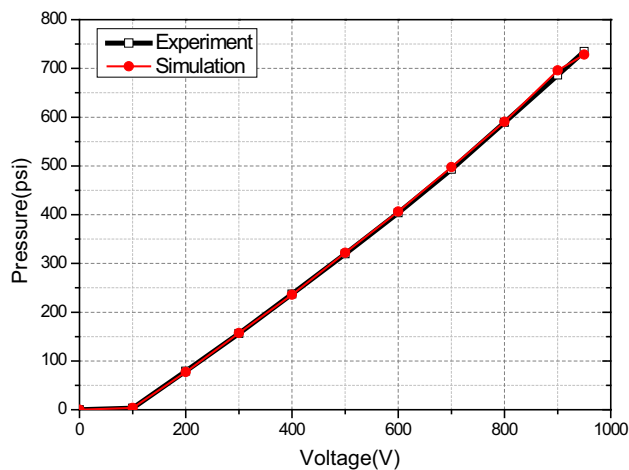


Fig. 12 Relationship between voltage and pressure (experiment vs simulation)

As shown in Fig. 12, it was found that the ratio of input voltage versus load pressure had linearity. The input voltage and the output pressure had an accurate ratio in the high voltage section, but the pressure formation hardly occurred in the low voltage section of 100 V or less. From Figs. 11 and 12, it was confirmed that the AMESim modeling of the small piezoelectric-hydraulic pump was done properly. In addition, in the future, a comprehensive investigation into modeling should pave the way for the development of a lightweight small piezoelectric-hydraulic pump with improved performance.

5 Conclusions

In this study, a small piezoelectric-hydraulic pump suitable for the braking system of small- and medium-sized UAVs was developed. In addition, the pressurization characteristics of the pump were analyzed and performance experiments of the developed pump were conducted. To analyze the pressurization characteristics of the small piezoelectric-hydraulic pump, the AMESim program was used. The hydraulic pump in its entirety, including the piezoelectric actuator, chamber, check valves, and load side, was modeled. To elaborately model the dynamic characteristics of the check valves in the AMESim program, a technical model rather than single components was constructed. The flow path through the check valve to the solenoid valve was also modeled with a pipeline rather than a simple flow path to obtain more accurate simulation results. Furthermore, the validity of the analytical modeling was verified by comparing the analysis results with the performance experimental results of the manufactured pump.

Experiments on the no-load exhaust flow rate, the hydraulic pressure at the load side behind the exhaust part,

and the pressurization speed of the piezoelectric-hydraulic pump showed that the maximum exhaust flow rate was 205 cc/min at 140 Hz, the maximum load pressure was 750 psi at 130 Hz, and the time to reach the normal operating pressure (450 psi) required for braking operation was within about 30 ms. It was concluded that these results satisfied the pump requirements. Comparing the experimental results of the pressure formation process with the simulation results, there was a slight difference in values during the pressurization stage. This occurred because the fluid structure interaction (FSI) dynamic behavior of the check valve and its shape were not considered in the model. In this study, it was nevertheless confirmed that the pressurization characteristics modeling of the developed small piezoelectric-hydraulic pump was carried out appropriately.

Acknowledgements The present study was supported by the Research Fund Support for Basic Research provided by the Agency for Defense Development (ADD-IBR-227). The authors would also like to thank the related individuals for their support.

References

1. Ma HK, Hou BR, Wu HY, Lin CY, Gao JJ, Kou MC (2008) Development and application of a diaphragm micro-pump with piezoelectric device. *J Microsyst Technol* 14(7):1001–1007
2. Junwu K, Zhigang Y, Taijiang P, Guangming C, Wu B (2005) Design and test of a high-performance piezoelectric micropump for drug delivery. *J Sens Actuators A Phys* 121(1):156–161
3. Larson JP, Dapino MJ (2012) Reliable, high-frequency miniature valves for smart material electrohydraulic actuators. *J Intell Mater Syst Struct* 23(7):805–813
4. Ham YB, Oh SJ, Seo WS, Park JH, Yun SN (2009) A piezoelectric micropump for microscale pumping systems. *J Drive Control* 36(2):17–25
5. Laser DJ, Santiago JG (2004) A review of micropumps. *J Micromech Microeng* 14(6):35–64
6. Iverson BD, Garimella SV (2008) Recent advances in microscale pumping technologies: a review and evaluation. *J Microfluid Nanofluid* 5(2):145–174
7. Chaudhuri A, Wereley N (2012) Compact hybrid electrohydraulic actuators using smart material: a review. *J Intell Mater Syst Struct* 23(6):597–634
8. Joo YH, Hwang J, Bae J, Yang J, Kwon J (2014) The design on the spring sheet type check valve of smart material hydraulic pump. In: *The society for aerospace system engineering, Fall Conference Paper #85*, 2014
9. Lee J, Hwang J, Yang J, Joo Y, Bae J, Kwon J (2015) Design of the compound smart material pump for brake system of small. Medium size UAV. *J Soc Aeronaut Syst Eng* 9(3):1–7
10. Hwang J, Lee J, Hwang J, Bae J, Kwon J (2014) Conceptual design of compound smart material pump with sequential operation of fluid displacement-force. In: *The society for aerospace system engineering, Spring Conference Paper #95*, 2014
11. Joo YH, Hwang JH, Yang JY, Bae JS, Kwon JY (2015) On the performance test of the piezoelectric-hydraulic pump. *J Korean Soc Aeronaut Space Sci* 43(9):706–711
12. Lee JH, Yum HH, Hong MS (2012) A study on the Antiabrasion of the aircraft carbon disk brake. *J Korean Soc Manuf Technol Eng* 21(6):968–975

13. FAA-H-8083-1A (2007) Aircraft weight and balance handbook. U. S. Department of Transportation, Federal Aviation Administration, Flight Standards Service, 2007
14. FAA-H-8083-30 (2008) Aviation maintenance technical handbook. U. S. Department of Transportation, Federal Aviation Administration, Flight Standards Service, 2008
15. Pazmany L (1986) Landing gear design for light aircraft. *Pazmany Aircr Corp* 1:14–15
16. Limpert R (1992) Brake design and safety. Society of Automotive Engineers. Warrendale, PA, pp 255–258
17. Xuan Z, Jin T, Ha NS, Goo NS, Kim TH, Bae BW, Ko HS, Yoon KW (2014) Performance of piezo-stacks for a piezoelectric hybrid actuator by experiments. *J Intell Mater Syst Struct* 25(18):2212–2220
18. Sirohi J, Chopra I (2003) Design and development of a high pumping frequency piezoelectric-hydraulic hybrid actuator. *J Intell Mater Syst Struct* 14(3):135–147